Available online at www.sciencedirect.com

SciVerse ScienceDirect

Ceramics International 39 (2013) 6131–6137

CERAMICS INTERNATIONAL

www.elsevier.com/locate/ceramint

Synthesis and growth of SiC/SiO_2 nanocables decorated with laminated porous ceramics from filter paper and polymeric precursor

Jianmei Pan[a], Xiaonong Cheng[a,*], Xuehua Yan[a], Jianfeng Pan[b], Chenghua Zhang[a], Qingbo Lu[b]

[a]School of Materials Science and Engineering, Jiangsu University, Zhenjiang 212013, PR China
[b]School of Energy and Power Engineering, Jiangsu University, Zhenjiang 212013, PR China

Received 13 December 2012; received in revised form 10 January 2013; accepted 10 January 2013
Available online 29 January 2013

Abstract

A simple and efficient way to synthesize the SiC/SiO_2 nanocables decorated with the laminated porous ceramics by pyrolysis of filter papers impregnated with silicone resins in flowing argon atmosphere has been successfully developed. The phase composition of the laminated porous ceramics was measured by X-ray diffraction. The morphology and microstructure of the samples were analyzed by scanning electron microscopy and transmission electron microscopy. The experimental results show that the nanocables composed of crystalline SiC core coated with a shell of amorphous SiO_2 were observed in the interfacial channels and pores of the laminated ceramics. The diameters of SiC cores were 40–80 nm and the thicknesses of SiO_2 shells were 4–10 nm. The increase of the pyrolysis temperature caused an increase in the amount of SiC/SiO_2 nanocables. Finally, a vapor–liquid–solid (VLS) process was discussed as the growth mechanism of the nanocables.

Keywords: A. Calcination; $SiC–SiO_2$ nanocables; Polymeric precursor; Vapor–liquid–solid process

1. Introduction

SiC nanomaterials such as wires, rods, belts, tubes, and cables have attracted tremendous attention recently due to their excellent properties and unique applications in nanoscale devices [1–3]. Especially, SiC nanowires not only possess better mechanical properties than those of bulk SiC [4], but also exhibit good field-emitting properties, chemical stability and thermal shock resistance [5–7]. Therefore, SiC nanowires have great potential as reinforcement material in ceramics, metals and polymers. SiC/SiO_2 nanocables, composed of a crystalline SiC core and amorphous SiO_2 shell, are ideal semiconductor–insulator heterostructures and have the features of both nanowires and nanotubes [8–11]. In the past several years, various synthetic approaches for preparing SiC nanostructures have been explored, mainly including laser ablation, carbon thermal reduction, physical evaporation, arc discharge, and chemical vapor deposition (CVD) [4,12–14]. However, most previous approaches required vacuum environment, high-grade equipments, and high temperature. Therefore, it is meaningful to develop a simple and low cost method for the production of SiC nanomaterials.

Recently, novel and simple processing techniques have been developed for the production of porous ceramics obtained from silicon-containing polymeric precursors [15–19] and SiC nanomaterials were observed in the porous ceramics. It is well known that polymeric precursors are also the valuable sources for the growth of one-dimensional (1D) nanomaterials under appropriate conditions [20–24]. These polymeric precursors for preparing nanomaterials mainly include polysiloxanes (PSX), poly (dimethyl siloxane) (PDMS), polycarbosilanes (PCS), polysilanes, polysilazanes (PSZ), and poly(methyl–phenyl) silsesquioxane (PMPSSX). Generally, the formation of

*Correspondence to. School of Materials Science and Engineering, Jiangsu University, No. 301 Xuefu Road, Zhenjiang 212013, PR China. Tel.: +86 511 88780006; fax: +86 511 88791739.
E-mail address: xncheng@ujs.edu.cn (X. Cheng).

0272-8842/$ - see front matter © 2013 Elsevier Ltd and Techna Group S.r.l. All rights reserved.
http://dx.doi.org/10.1016/j.ceramint.2013.01.031

1D nanomaterials from polymeric precursors is facilitated by a transition metal as a catalyst source (Fe, Ni, Co, Cr, etc.) [25–27]. For example, Fu et al. [9] synthesized well-aligned Si_3N_4/SiO_2 coaxial nanocables by pyrolysis of a preceramic polymer (perhydropolysilazane) with iron. Cai et al. [10] prepared SiC/SiO_2 nanocables by pyrolysis of poly(dimethyl siloxane) using ferrocene as a metal catalyst. So far, little work has been done on the synthesis of SiC/SiO_2 nanocables from polymeric precursors.

In this work, SiC/SiO_2 nanocables decorated with laminated porous silicon oxycarbide (SiOC) ceramics were prepared by pyrolysis at low temperatures, using cellulosic material (filter paper) as a biomorphic template, and silicone resin was applied as a polymeric precursor. This is an efficient, simple and economical route to synthesize SiC/SiO_2 nanocables. In our experiments, the effects of the pyrolysis temperature on the microstructure and morphology of the as-prepared samples were investigated. Furthermore, the growth mechanism of SiC/SiO_2 nanocables was proposed.

2. Experimental section

Filter paper (Hangzhou Xinhua Paper Industry Co., Ltd., Zhejiang, China) was used as a biomorphic template. Commercially available silicone resin (solid content: 48–52%, Tu-4 cup viscosity at 25 °C: 18–35 s, Changzhou Jianuo Organosilicon Co., Ltd., Jiangsu, China) was used as a polymeric precursor. The mass ratio of silicone resin to filter paper was 2:1, using xylene as a solvent. The silicone resins were adequately absorbed in the filter papers, and then were dried at 85 °C for 12 h under drying oven. The filter papers impregnated with silicone resins were molded using hot-pressing equipment under a pressure of 40 MPa at 80 °C for 20 min. The pyrolysis of the samples was carried out in a tube furnace in Ar (99.95%) atmosphere at a rate of 0.25 L/min, in a multi-step-heating schedule. The green bodies were first heated with a heating ramp of 5 °C/min up to 150 °C and kept constant for 15 min. Then on a second ramp, the green bodies were heated at 2 °C/min up to 400 °C and kept at this temperature for 30 min. Then on a third ramp, the green bodies were heated at 5 °C/min up to a set temperature (1200 °C and 1300 °C), keeping the sample at this temperature for 180 min. Finally, the samples were cooled down to room temperature at 3 °C/min.

The elemental composition of filter paper was analyzed by means of inductively coupled plasma-optical emission spectrometry (ICP-OES, Vista-MPX, America). The morphology and elemental composition of the samples were examined using a scanning electron microscope (SEM, JSM-7001F, Japan) equipped with a energy dispersive spectrometer (EDS). The microstructure of the samples was further characterized by a field emission transmission electron microscope (TEM, JEOL-2010, Japan), and energy-dispersive X-ray spectroscopy (EDX) (attached to the TEM). TEM samples were gently ground with an agate mortar for a few seconds and then dispersed in ethanol by ultrasonic vibrations for 3 h before being dropped on a copper grid coated with carbon film.

3. Results and discussion

In order to analyze the thermal decomposition behaviors of filter paper and filter paper/silicone resin, TG curves under argon atmosphere are shown in Fig. 1. It can be found that the thermal decomposition of the filter paper includes three stages, as shown in Fig. 1a. A weight loss of 4.5 wt% at the first stage (20–270 °C) was due to the desorption of physically adsorbed water. At the second stage, a higher weight loss of 81.1 wt% in the range of 270–390 °C was due to the depolymerization of cellulosic, carbonation reaction, and the release of volatile matters (H_2O, CO_2, CO) [28]. At the last stage, the filter paper displayed a weight loss of 12.7 wt% attributed to a further

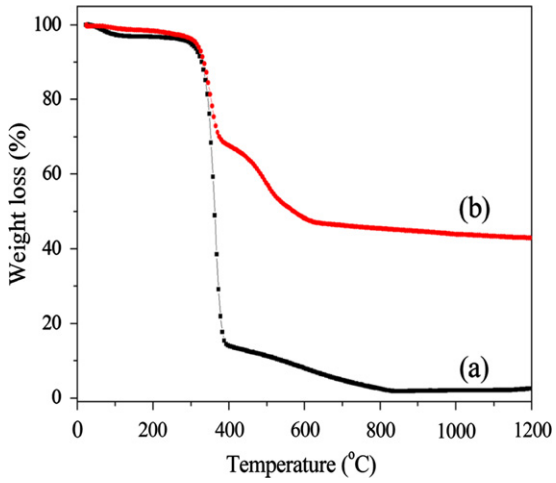

Fig. 1. TG curves of the filter paper (a) and filter paper/silicone resin (b).

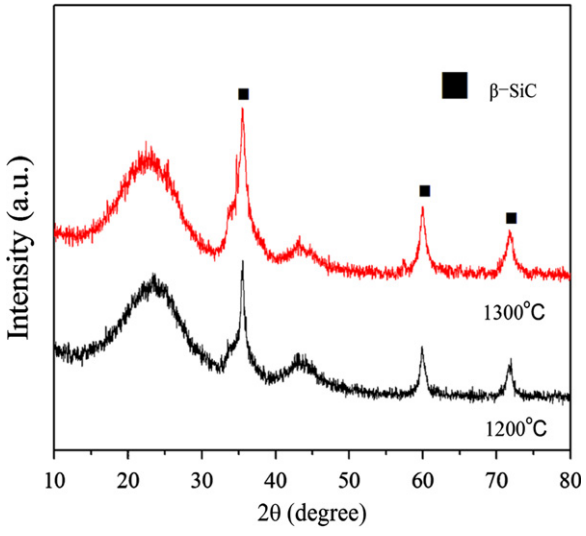

Fig. 2. XRD patterns of the laminated porous ceramics at different temperatures.

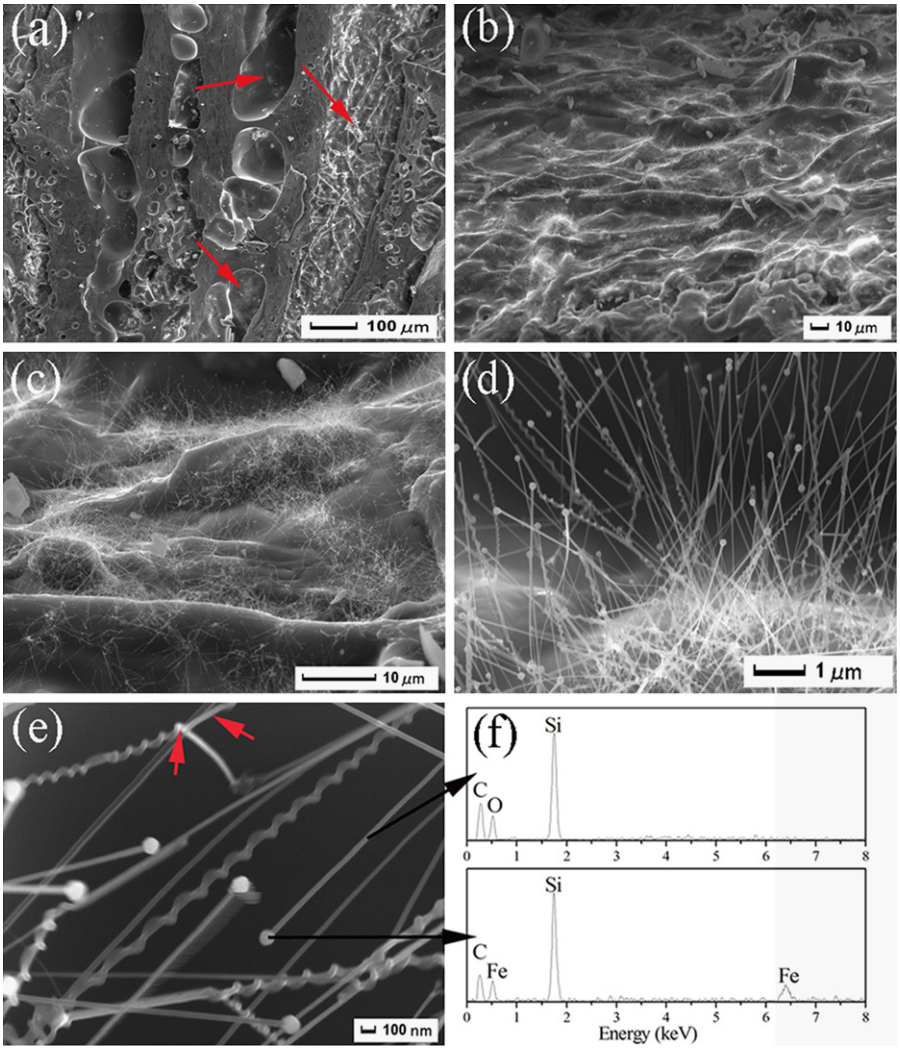

Fig. 3. SEM image of the fracture surface of the laminated porous ceramic at 1200 °C (a); SEM image of the wire-like products on the surface of the fibers derived from filter paper (b); typical images of the wire-like products (c) and (d); high-magnification SEM image of the wire-like products (e); EDS spectrum (upper right) taken from the nanowire and EDS spectrum (lower right) taken from the attached particle (f).

carbonation process. It can be found that the filter paper was completely pyrolyzed at 840 °C. After filter paper was impregnated with silicone resin, the thermal decomposition behavior was shown in Fig. 1b. The initial weight loss of 3.5 wt% was observed in the range of 20–290 °C due to the desorption of physically adsorbed water. At the second stage (290–618 °C), the weight loss of 49.2 wt% was attributed to the pyrolysis of filter paper, degradation reactions of the Si–O polymer chain, and the release of volatile matters. It can be noted that a weight loss of 4.3 wt% in the last step (610–1200 °C) was due to a further carbonation of filter paper and redistribution reactions of different silicon sites.

Fig. 2 shows the XRD patterns of the as-prepared samples at different temperatures. It should be mentioned that the broad diffraction peak at 21–23° is associated with the Si–O–C glass. It is well accepted that polysiloxanes were converted into amorphous SiOC glasses between 800 °C and 1300 °C [29]. The weak diffraction peak at 43° associated with the disorder carbon layer corresponds to the diffraction line from the (10l) lattice plane of the graphite (JCPDS Card no. 01-0646). It can be concluded that the carbon sheets with low graphitization degree were formed due to the thermal decomposition of the cellulose and silicone resin. The XRD patterns of the samples show the diffraction peaks at 2θ of 35.93°, 60.37° and 71.99°. These peaks are in agreement with the reflection of the (111), (220) and (311) planes of β-SiC (JCPDS Card no. 29-1129). Additionally, it can be found that the intensity of the peaks of β-SiC increases with increasing temperature.

Fig. 3a shows the fracture surface of the laminated porous ceramic obtained at 1200 °C. The as-prepared porous sample contains 46% porosity. It can be noted that the wire-like products were formed inside the pores and interfacial channels (individual layer), as indicated by arrows. Fig. 3b shows the low-magnification image of individual layer. It can be found that an interesting morphology of the wire-like products was observed on

the surface of the fibers from filter paper. Fig. 3c and d shows the typical images of the wire-like products, indicating that the wire-like products display different morphologies with straight and spiral-like structures. And the spiral-like products were coiled up on the straight wire-like products. Furthermore, the spherical particles were found on the tips of the wire-like products. Fig. 3e shows the high-magnification SEM image of the wire-like products, suggesting that the diameters of these wire-like products range from 50 to 100 nm and the lengths are up to several micrometers. A typical EDS spectrum in Fig. 3f indicates that the wire-like products contain Si, C, and O in a 46.3:40.1:13.6 atomic ratio. The three elements coexisting strongly suggest that the wire-like products may be formed SiC/SiO_2 core–shell nanocables, which is also proved by later TEM observation. The EDS spectrum of the spherical particle shows the peaks associated with iron (Fe). Fig. 4 shows the fracture surface of the laminated porous ceramic obtained at 1300 °C. The as-prepared porous sample contains 55% porosity. It can be found that a large amount of wire-like products were formed inside the pores and individual layer, as indicated by arrows in Fig. 4a. No significant change was observed in the general morphology of the wire-like products heated in the 1200–1300 °C temperature range (Fig. 4b and c). In addition, increasing the pyrolysis temperature caused an increase in the amount of the wire-like materials produced.

In order to analyze the source and content of Fe element, the ICP-OES results for the elemental composition of the filter paper are listed in Table 1. Other elements can be neglected due to their weak intensity during the ICP-OES measurement. Apparently, the filter paper possesses a rather low Fe content.

Further characterization of the wire-like products synthetized at 1200 °C was conducted using TEM and HRTEM analysis, as shown in Fig. 5. Fig. 5a shows a typical TEM image of the wire-like products, indicating

Table 1
Elemental composition of the filter paper.

Elements	Mg	Si	Ca	Fe
mg/g	0.04	0.075	0.25	0.026

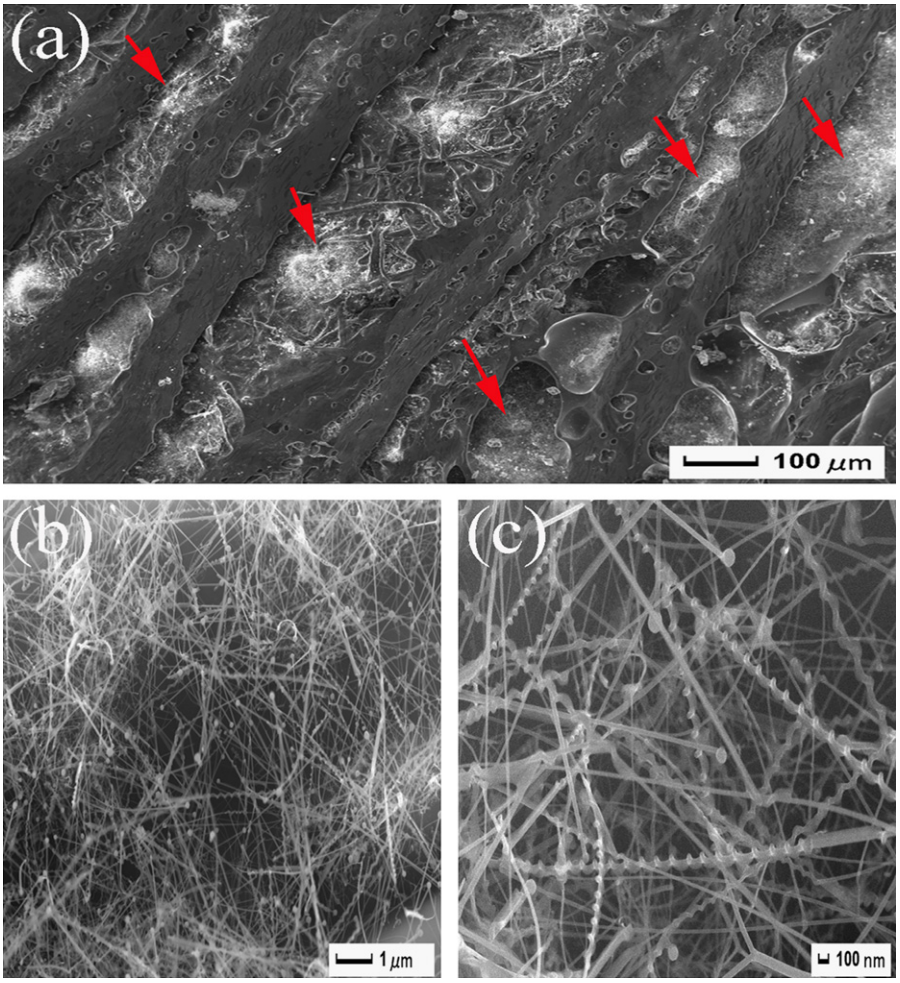

Fig. 4. SEM image of the fracture surface of the laminated porous ceramic at 1300 °C (a); and high-magnification SEM images of the wire-like products (b) and (c).

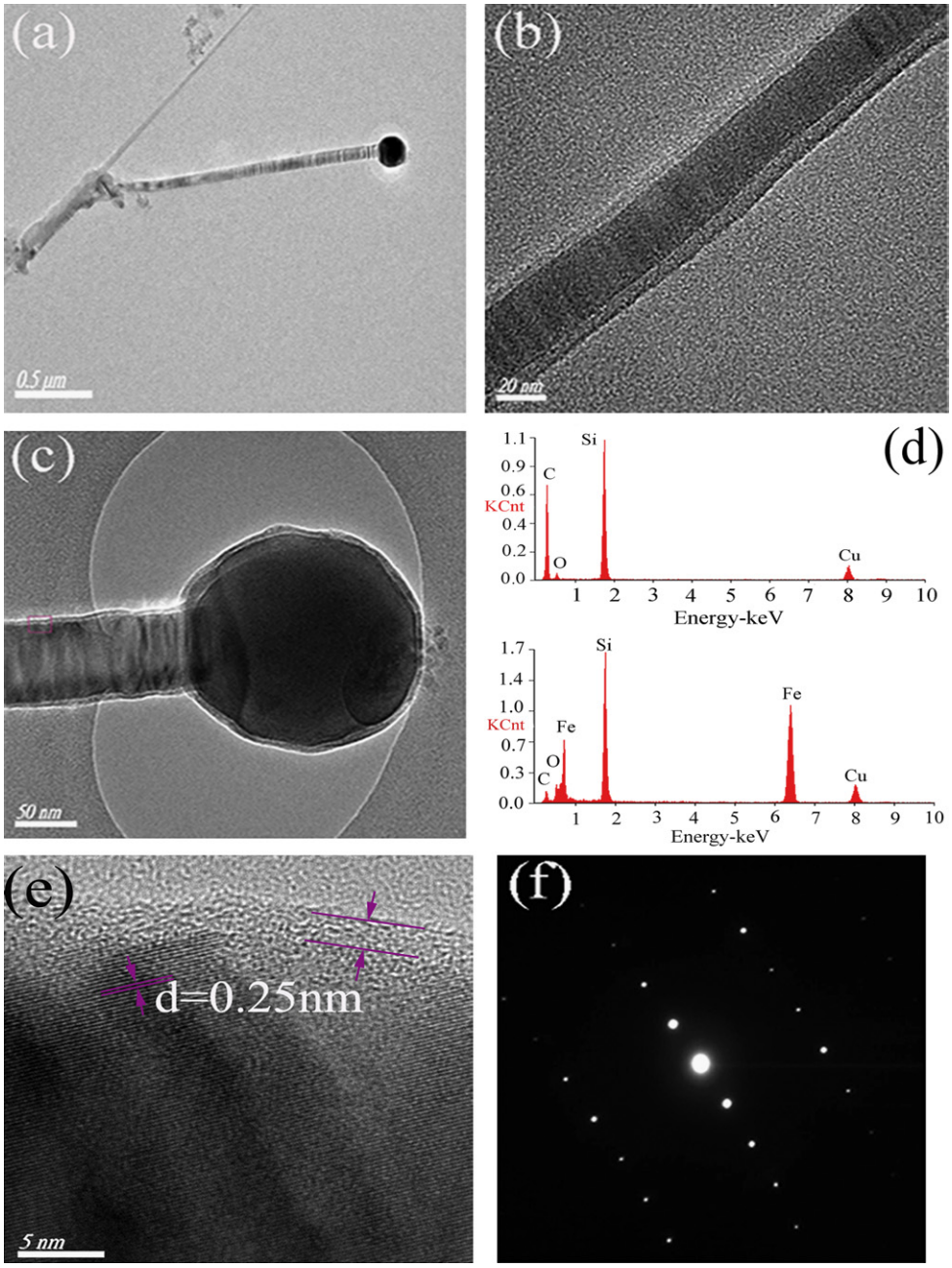

Fig. 5. A typical TEM image of the wire-like products (a); low-magnification TEM images of the nanocables (b) and (c); EDX spectrum (upper right) taken from the wire stem of the nanocable and EDX spectrum (lower right) taken from the attached particle (d); HRTEM image of the nanocable (e); and SAED pattern taken from the core of the nanocable (f).

that the wire-like product has a metal catalyst particle. Fig. 5b and c shows the high-magnification TEM image of the wire-like products. It is interesting to note that the wire-like products have a core–shell structure. And the core–shell structure consists of an inner core of 40–80 nm diameter and a light outer shell of 4–10 nm thickness. Fig. 5d shows the EDX spectra taken from the wire stem and attached particle of the nanocable. The EDX spectrum (upper right) from the wire stem of the nanocable shows that the wire contains C, Si, and O. The EDX spectrum (lower right) from the attached particle reveals that the particle contains Fe, C, Si, and O, which is the obvious evidence of VLS growth process. The presence of Cu seen in the EDS spectra is likely due to the Cu TEM grid used to affix the sample. It can be concluded that Fe element derived from filter paper results in the formation of the metal catalyst for the growth of the nanocables. Fig. 5e displays a typical HRTEM image of the rectangular area (Fig. 5c), in which well-defined fringe separation of 0.25 nm is consistent with the *d*-spacing of (111) plane, indicating that SiC nanowires grow along the [111] direction. HRTEM image clearly shows that the core of the nanocable is structurally uniform, and has no obvious stacking faults or twins. It can be

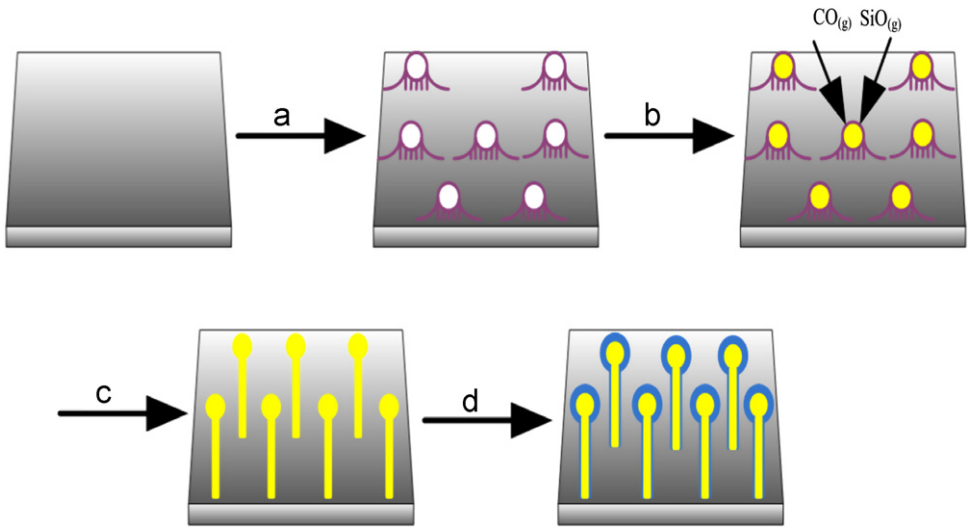

Fig. 6. Schematic illustrations for the proposed growth model of SiC/SiO_2 nanocables. Formation of the iron droplets (a); formation of the liquid Fe–Si–C–O alloys and diffusion of gaseous SiO and CO surrounding the alloys (b); formation of SiC nanowires (c); and formation of SiC/SiO_2 nanocables (d).

concluded that the shell of the nanocable is the amorphous SiO_2 identified by HRTEM image and component ratio obtained by EDX result. Fig. 5f displays the corresponding SAED pattern of the core of the nanocable, indicating that the core of the nanocable is a single crystal of cubic SiC. Based on TEM analysis, it can be demonstrated that the as-synthesized wire-like product has a core–shell nanostructure with a single-crystalline β-SiC core and an amorphous SiO_2 outer shell.

It is well established that the metal catalysts are frequently used for the synthesis of the nanostructures. It is clearly seen that there is a nanoparticle on the tip of the nanocable, which is commonly considered to be evidence of vapor–liquid–solid (VLS) mechanism for the growth of 1D nanostructures. The VLS mechanism for the growth of the nanocables initiated by a metal catalyst has been suggested [26,27]. Based on the literature and analysis from SEM and TEM, the formation process of the nanocables could be rationally comprehended by a tip growth model (VLS mechanism), as illustrated in Fig. 6. The growth process may consist of the following steps. The initial step is the formation of the catalytic particles through the precipitation process at a high temperature. During the pyrolysis process, the small-molecule gases (CH_4, C_2H_6, H_2) were created, which were attributed to the cleavage of the polymer chain and the decomposition of methyl groups [30]. The iron-compounds from filter paper were reduced by H_2 to form atomic irons, which were agglomerated into the iron droplets at high temperature. The second step is the evolution of SiO and CO gases derived from the pyrolysis of the silicone resin and filter paper, and the redistribution reaction of the Si sites. The SiO vapor and amorphous carbon were absorbed and dissolved in the liquid-iron droplets to form a liquid Fe–Si–C–O alloy, as observed in other studies [11]. The liquid alloy surface has a large accommodation coefficient, which is a preferable site for the incoming gaseous SiO and CO gases. Subsequently, SiC nanowires were formed via a gas–gas reaction, as shown below in Eq. (1). Then CO_2 further reacted with solid C via reaction (2) to form CO, and the overall reaction (3) is written as follows. Lastly, when the Fe–Si–O–C alloy droplets become supersaturated, the amorphous SiO_2 was separated out continuously to form the shell via reaction (4). During the growth process, the existence of oxygen in the tube should also be considered for the formation of the amorphous SiO_2. Reaction (5) of SiO gas with oxygen is written as follows:

$$SiO_{(g)} + 3CO_{(g)} \rightarrow SiC_{(s)} + 2CO_{2(s)} \quad (1)$$

$$C_{(s)} + CO_{2(g)} \rightarrow 2CO_{(g)} \quad (2)$$

$$SiO_{(g)} + C_{(s)} \rightarrow SiC_{(s)} + CO_{(g)} \quad (3)$$

$$2SiO_{(g)} + C_{(s)} \rightarrow SiC_{(s)} + SiO_{2(s)} \quad (4)$$

$$2SiO_{(g)} + O_{2(g)} \rightarrow 2SiO_{2(s)} \quad (5)$$

4. Conclusions

SiC/SiO_2 core–shell nanocables decorated with laminated porous SiOC ceramics were successfully fabricated by pyrolysis of filter paper impregnated with silicone resin under argon atmosphere. SiC/SiO_2 nanocables were observed in the interfacial channels and pores of the porous ceramics. The diameters of the nanocables are in the range of 50–100 nm and the lengths are up to several micrometers, and SiO_2 shells of the nanocables are in the range of 4–10 nm. The iron element derived from filter paper results in the formation of metal catalyst for the growth of nanocables. The growth process of the nanocables is controlled by the VLS mechanism.

Acknowledgments

This work was supported by the Materials Tribology Key Laboratory of Jiangsu Opening Foundation (kjsmcx07005), the Natural Science Foundation of the Jiangsu High Education (08KJD430010), the Postgraduate Research and Innovation Project of Ordinary University in Jiangsu Province (CXZZ11_0558), the Talent Foundation of Jiangsu University (09jdg033), Changshu Research Project (CG201005) and the Excellent Young Teacher of Jiangsu for financial support.

References

[1] E.W. Wong, P.E. Sheehan, C.M. Lieber, E.W. Wong, P.E. Sheehan, C.M. Lieber, Nanobeam mechanics: elasticity, strength and toughness of nanorods and nanotubes, Science 277 (1997) 1971–1975.
[2] B.H. Yan, G. Zhou, W.H. Duan, J. Wu, B.L. Gu, Uniaxial-stress effects on electronic properties of silicon carbide nanowires, Applied Physics Letters 89 (2006) 023104–023106.
[3] H.K. Seong, H.J. Choi, S.K. Lee, J.I. Lee, D.J. Choi, Optical and electrical transport properties in silicon carbide nanowires, Applied Physics Letters 85 (2004) 1256–1258.
[4] H.J. Dai, E.W. Wong, Y.Z. Lu, S.S. Fan, C.M. Lieber, Synthesis and characterization of carbide nanorods, Nature 375 (1995) 769–772.
[5] W.M. Zhou, Y.J. Wu, E.S.W. Kong, F. Zhu, Z.Y. Hou, Y.F. Zhang, Field emission from nonaligned SiC nanowires, Applied Surface Science 253 (2006) 2056–2058.
[6] H.W. Shim, J.D. Kuppers, H. Huang, High-temperature stability of silicon carbide nanowires, Journal of Nanoscience and Nanotechnology 8 (2008) 3999–4002.
[7] G.Z. Shen, Y. Bando, C.H. Ye, B.D. Liu, D. Golberg, Synthesis, characterization and field-emission properties of bamboo-like β-SiC nanowires, Nanotechnology 17 (2006) 3468–3472.
[8] Y. Ryu, Y. Tak, K. Yong, Direct growth of core–shell SiC–SiO_2 nanowires and field emission characteristics, Nanotechnology 16 (2005) S370–S374.
[9] X.L. Fu, Z.J. Peng, N. Zhu, C.B. Wang, Z.Q. Fu, L.H. Qi, H.Z. Miao, Aligned Si_3N_4@SiO_2 coaxial nanocables derived from a polymeric precursor, Nanotechnology 21 (2010) 245603–245609.
[10] K.F. Cai, A.X. Zhang, J.L. Yin, Ultra thin and ultra long SiC/SiO_2 nanocables from catalytic pyrolysis of poly(dimethyl siloxane), Nanotechnology 18 (2007) 485601–485606.
[11] A. Meng, Z.J. Li, J.L. Zhang, L. Gao, H.J. Li, Synthesis and Raman scattering of β-SiC/SiO_2 core–shell nanowires, Journal of Crystal Growth 308 (2007) 263–268.
[12] K.W. Wong, X.T. Zhou, F.C.K. Au, H.L. Lai, C.S. Lee, S.T. Lee, Field-emission characteristics of SiC nanowires prepared by chemical-vapor deposition, Applied Physics Letters 75 (1999) 2918–2920.
[13] Y. Zhang, K. Suenaga, C. Colliex, S. Lijima, Coaxial nanocable: silicon carbide and silicon oxide sheathed with boron nitride and carbon, Science 281 (1998) 973–975.
[14] S.C. Chiu, C.W. Huang, Y.Y. Li, Synthesis of high-purity silicon carbide nanowires by a catalyst-free arc-discharge method, Journal of Physical Chemistry C 111 (2007) 10294–10297.
[15] C. Zollfrank, R. Kladny, H. Sieber, P. Greil, Biomorphous SiOC/C-ceramic composites from chemically modified wood templates, Journal of the European Ceramic Society 24 (2004) 479–487.
[16] Y.L. Li, H. Fan, D. Su, C. Fasel, R. Riedel, Synthesis, structures, and properties of bulk Si(O)C ceramics from polycarbosilane, Journal of the American Ceramic Society 92 (2009) 2175–2181.
[17] R. Riedel, M. Seher, J. Mayer, D. Vinga-Szabó, Polymer-derived Si-based bulk ceramics, part I: preparation, processing and properties, Journal of the European Ceramic Society 15 (1995) 703–715.
[18] P. Colombo, G. Mera, R. Riedel, G.D. Sorarù, Polymer-derived ceramics: 40 years of research and innovation in advanced ceramics, Journal of the American Ceramic Society 93 (2010) 1805–1837.
[19] J.M. Pan, X.H. Yan, X.N. Cheng, Q.B. Lu, M.S. Wang, C.H. Zhang, Preparation of SiC nanowires-filled cellular SiCO ceramics from polymeric precursor, Ceramics International 38 (2012) 6823–6829.
[20] C.Y. Wan, G.C. Guo, Q.S. Zhang, SiOC ceramic nanotubes of ultrahigh surface area, Materials Letters 62 (2008) 2776–2778.
[21] M. Scheffler, P. Greil, A. Berger, E. Pippel, J. Woltersdorf, Nickel-catalyzed in situ formation of carbon nanotubes and turbostratic carbon in polymer-derived ceramics, Materials Chemistry and Physics 84 (2004) 131–139.
[22] H. Wang, X.D. Li, T.S. Kim, D.P. Kim, Inorganic polymer-derived tubular SiC arrays from sacrificial alumina templates, Applied Physics Letters 86 (2005) 173104–173106.
[23] Y. Fan, Y.S. Wang, J.S. Lou, S.F. Xu, L.G. Zhang, L.N. An, H. Heinrich, Formation of silicon-doped boron nitride bamboo structures via pyrolysis of a polymeric precursor, Journal of the American Ceramic Society 89 (2006) 740–742.
[24] X.D. Zhang, X.X. Huang, G.W. Wen, X. Geng, J.D. Zhu, T. Zhang, H. Bai, Novel SiOC nanocomposites for high-yield preparation of ultra-large-scale SiC nanowires, Nanotechnology 21 (2010) 385601–385608.
[25] W.Y. Yang, F.M. Gao, H.T. Wang, X.M. Zheng, Z.P. Xie, L.A. An, Synthesis of ceramic nanocomposite powders with in situ formation of nanowires/nanobelts, Journal of the American Ceramic Society 91 (2008) 1312–1315.
[26] C. Vakifahmetoglu, E. Pippel, J. Woltersdorf, P. Colombo, Growth of one-dimensional nanostructures in porous polymer-derived ceramics by catalyst-assisted pyrolysis. Part I: iron catalyst, Journal of the American Ceramic Society 93 (2010) 959–968.
[27] C. Vakifahmetoglu, P. Colombo, S.M. Carturan, E. Pippel, J. Woltersdorf, Growth of one-dimensional nanostructures in porous polymer-derived ceramics by catalyst-assisted pyrolysis. Part II: cobalt catalyst, Journal of the American Ceramic Society 93 (2010) 3709–3719.
[28] Z.Y. Luo, S.R. Wang, Y.F. Liao, K.F. Cen, Mechanism study of cellulose rapid pyrolysis, Industrial & Engineering Chemistry Research 43 (2004) 5605–5610.
[29] H.J. Kleebe, C. Turquat, G.D. Sorarù, Phase separation in an SiCO glass studied by transmission electron microscopy and electron energy-loss spectroscopy, Journal of the American Ceramic Society 84 (2001) 1073–1080.
[30] J.L. Plawsky, F. Wang, W.N. Gill, Kinetic model for the pyrolysis of polysiloxane polymers to ceramic composites, AIChE Journal 48 (2002) 2315–2323.